Central European Journal of Energetic Materials
ISSN 1733-7178; e-ISSN 2353-1843

Cent. Eur. J. Energ. Mater. 2023, *20*(4): 417-441; DOI 10.22211/cejem/173190
Article is available in PDF-format, in colour, at:
https://ipo.lukasiewicz.gov.pl/wydawnictwa/cejem-woluminy/vol-20-nr-4/

Research paper

On the Influence of the Liner Shape and Charge Detonation Scheme on the Kinetic Characteristics of Shaped Charge Jets and Explosively Formed Penetrators

Yuri Voitenko[1)], **Yuri Sydorenko**[2)], **Roman Zakusylo***[,3)], **Sergii Goshovskii**[2)], **Stefan Zaichenko**[2)], **Viktor Boyko**[1)]

[1)] *Institute of Hydromechanics, National Academy of Sciences of Ukraine, 03057 Kyiv, Ukraine*

[2)] *National Technical University of Ukraine "Igor Sikorsky Kyiv Polytechnic Institute", 03056 Kyiv, Ukraine*

[3)] *Shostka Institute of Sumy State University, 41100 Shostka, Ukraine*

* *E-mail:* r.zakusylo@ishostka.sumdu.edu.ua

ORCID information:
Zakusylo R.: 0000-0003-3823-4040

Abstract: The results of modelling the functioning of shaped charges with different liners and different detonation excitation schemes are presented. The simulation results are compared with experimental data and modelling results by other authors. The shaped charge explosion process was simulated with the help of the authors' program "Hephaestus" and the ANSYS/AUTODYN program. The results of determining the depth of penetration of cumulative jets into a barrier using the AV model (Allison and Vitali) are compared with experimental data. The dependence of the velocity of the leading part of the copper cumulative jet on the angle at the top of the conical liner is proposed. Attention was paid to the need to take into account the gradient of the properties of the liner material in the simulations.

Keywords: shaped charge, liner, shaped charge jets, explosively formed penetrators, penetration

1 Introduction

Shaped charges (SCs) are dual purpose devices. They are widely used in the military and civil spheres, in particular, to destroy armored vehicles, and to neutralize unexploded ordnance. SCs are used in oil and gas technology as well. In this paper, experimental data obtained on small-caliber shaped charges are compared with similar results, taking into account similarity theory relations. The similarity theory was applied to assess the reliability of numerical simulation methods and the possibility of their application to optimize the design of SCs.

An SC is an explosive device, the effectiveness of which is determined by the depth of penetration of a target by a shaped charge jet (SCJ). In addition, the efficiency is determined by the energy of the impact interaction between the target and the explosively formed penetrator (EFP), which is formed during the implosion of the liner. Over the past 15-20 years, the number of publications devoted to research into the functioning of SCs has increased markedly. This is due to the emergence of special software products. These software products allow computer simulation of SC explosion processes: explosive material (EM) detonation, deformation of the SC body, liner implosion with the formation of an SCJ or EFP, and penetration of the SCJ (EFP) into the barrier. In many cases, the results of calculations and the adequacy of the mathematical models describing the behaviour of materials under extreme conditions were tested experimentally or compared with other results [1-12]. A number of studies were devoted to the study of materials science aspects of the functioning of an SC [13-16]. An analysis of these studies [1-26] allows the main features of the SC design to be identified, which determine the depth of penetration of the barrier and the corresponding volume of the channel in it. These are dependent on the thickness, shape and material of the liner, the explosion energy of the explosive charge, and the charge detonation initiation scheme. In [2], quantitative estimates were obtained of the influence of individual geometric parameters of an SC or their combination on the penetration of a target. It was noted that the location of the detonation initiation point of the SC and the thickness of the liner have the greatest influence on the efficiency of the SC. The value of the angle at the top of the cone in the range of 44-46° and the distance to the target have much less influence. It should also be noted that there are two ideas for improving the efficiency of an SC, associated with a change in the mechanisms of implosion of the SC liners [9, 11]. An analysis of the process of implosion of a hemispherical liner of digressive thickness (the value of the liner thickness decreases from its top to the base) shows that the SC design creates a condition for liner compression close to spherically symmetry. Compression of the cladding leads to an increase

in the speed of the emerging jet flow and an increase in the manifestation of the effect of spherical cumulation. The SCJ mass-velocity parameters can approach the level of the SCJ parameters of conical liners, and when optimised could even exceed them. [9]. Paper [11] describes a different mechanism for the implosion of a conical lining, which differs from the mechanism for the implosion of charges of a traditional design (a cone, or shapes close to it). To do this, an additional element in the form of a special plate is placed in the cut-off top of the liner cone. When the oncoming flows are reflected from this plate, the liner material implosions occur at an angle greater than 180°. As a result, an SCJ is formed with a higher kinetic energy than can be obtained for an SCJ with the traditional scheme of conical liner implosion, which was confirmed by the results of modelling the operation of such a charge [12].

In article [17] the authors explored the influences of the angle at the top of the liner cone, the distance to the target and the length of the shaped charge on the efficiency of penetration into concrete targets. For this, conical liners were used in which the value of the angle at the top was 90°, 100° and 110° with an external charge diameter of 76 mm. The computer simulations in this study were performed using the LS-DYNA software. The simulation results showed that a cone angle of 90° leads to the formation of the longest SCJ, with the highest value of the lead velocity approximately 30-40 μs after the detonation of the explosive charge. The optimal distance to the barrier was from 70 to 100 mm, at which the jet could reach its maximum velocity and length.

The author of [27] conducted studies on the effect of the thickness of an aluminum liner and the angle at its top on the efficiency of breaking through the target. As the liner angle was increased from 100° to 120°, the SCJ penetration depth decreased, indicating a decrease in its speed, and as the liner thickness was increased from 2% to 8% of the SC caliber, the penetration depth increased.

In [13-15], the above factors and the influence of the location of the detonation excitation points, their number, barrier strength, initial temperature of the liner, and charge rotation speed were studied. Despite this, there are no systematic data in the literature on the mass-velocity parameters of SCJs, even for the simplest liner configurations: for a cone, a sphere, a spherical segment, and charges of different calibers. Therefore, the results of the research presented below will be able to augment the existing database on the velocities, masses of SCJs, and penetration depths of targets made of various materials.

Meaning practical applications of shaped charge explosions requires the availability of engineering evaluation methods or methods for calculating the mass-kinetic parameters of SCJs or EFPs, effective engineering methods for estimating the depth of penetration of an SCJ and SC into the barrier. In particular,

this concerns the solution of an urgent problem for Ukraine - the disposal of unused ammunition or the destruction of unused ammunition in the combat zone. Furthermore, research of this type is of great practical importance in the treatment of oil and gas reservoirs.

The purpose of this article is to verify the reliability of the results of mathematical modelling of the SC functioning by comparison with experimental data, and to study the effects of the liner shape and the detonation excitation scheme on the kinematic characteristics of SCJs and EFPs.

2 Materials and Methods of Research

2.1 Materials

Experimental studies of the process of functioning of SCs were carried out according to a well-known method, which is described in many publications [3, 6, 7, 13, 15]. The experimental samples of the liners were made from powdered copper PMS-N (GOST 4960-75). The mass of the liner in a charge of caliber 25.7 mm (Figure 1) was 14-15 g at a density of ≈7.8-8.1 g/cm^3. The porosity of the liner material was 10-29% and increased from the top of the liner (10-11%) to the bottom (28-29%). The mass of the liner in a charge of caliber 36.6 mm (Figures 2 and 3) was 34 g at the same density. In separate experiments, a charge with a liner of progressive thickness was also used, with a cone apex angle of 44°/48°. The mass of the liner was 15-18 g, the mass of the explosives was 18-19 g (Figure 4).

The SC charge was phlegmatized RDX with a density of 1.65 g/cm^3. The mass of the explosive in SCs of small caliber was 10 g, and of large caliber was 27-29 g. The detonation velocity was 7800-8100 m/s.

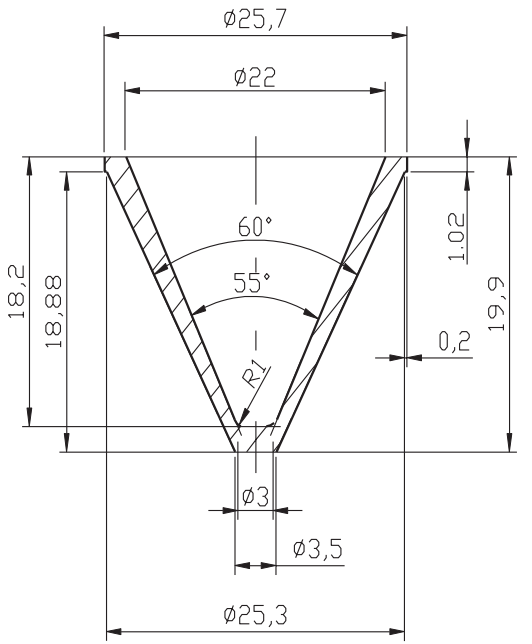

Figure 1. The design of the liner in a charge of small caliber

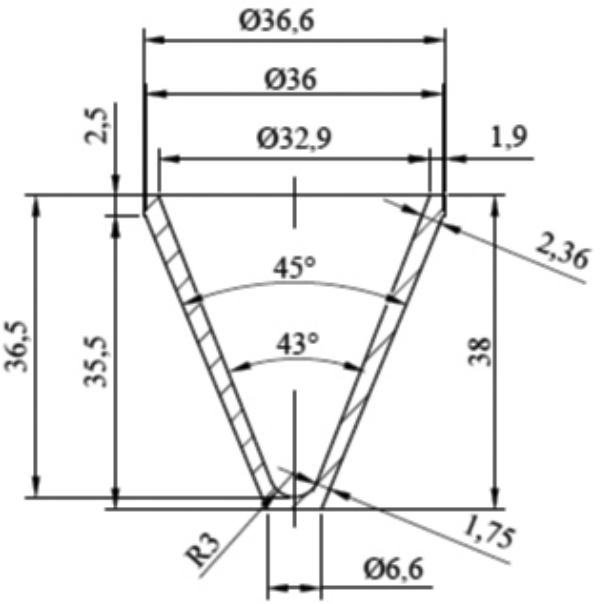

Figure 2. The design of the liner in a charge of a larger caliber

Figure 3. Experimental samples of the tested conical SCs

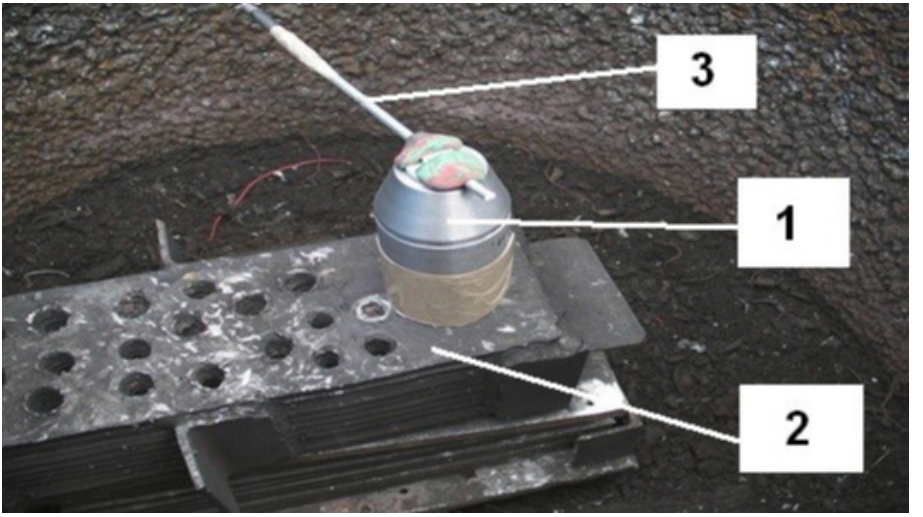

Figure 4. General view of the experimental set-up: charge (**1**), target (**2**) and detonating cord (**3**)

2.2 Simulation model

Mathematical studies of the process of the functioning of SCs were carried out in 4 structural schemes with a liner in the following forms:

– Cone with an angle at the top of 42°and wall thickness $\delta = 1.5$ mm (Figure 5),
– Progressive cone with angles at the top of 42°and 43°(Figure 6),
– Progressive cone with angles at the top of 55°and 60°(Figure 7),
– Spherical segment with an outer radius of 82.7 mm and $\delta = 2$ mm (Figure 8).

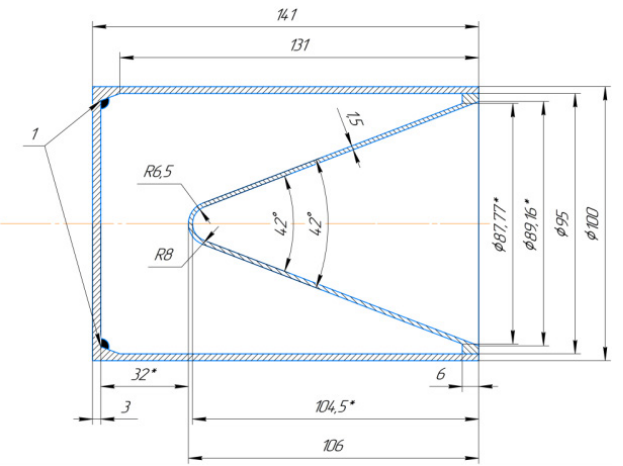

Figure 5. Scheme of an SC with a liner in the form of a cone with an angle at the top of 42°and a wall thickness of 1.5 mm

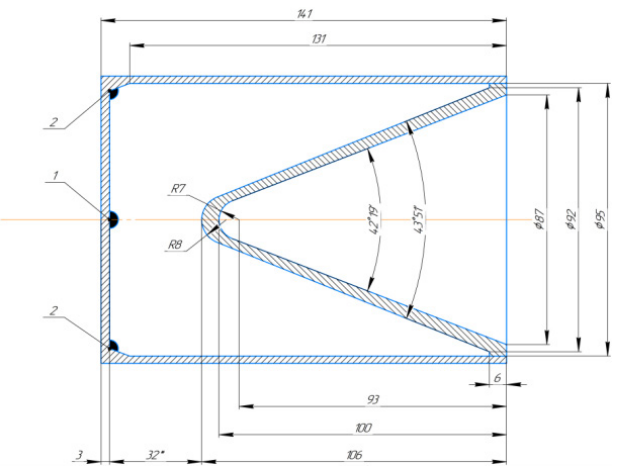

Figure 6. Scheme of an SC with a liner in the form of a cone with angles at the top 42°and 43° and progressive wall thickness

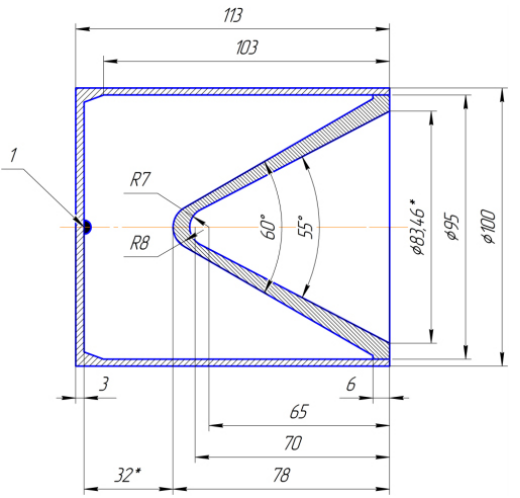

Figure 7. Scheme of an SC with a liner in the form of a cone with angles at the top 55°and 60° and progressive wall thickness

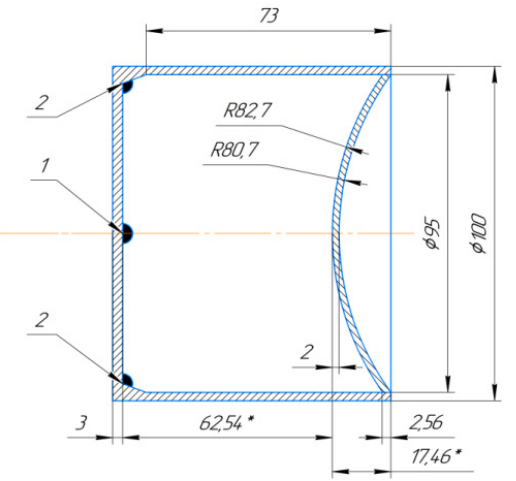

Figure 8. Scheme of an SC with a liner in the form of a spherical segment with an outer radius of 82.7 mm and a wall thickness of 2 mm

The main feature of all calculation schemes of shaped charges in Figures 5-8 is that:

– The structures have a cylindrical body with a wall thickness of 3 mm and a closed bottom.
– The diameter of the outer surface of the case is 100 mm.

– The distance from the inner end surface of the charge case to the liner is 32 mm, excluding the shaped charge scheme with a liner in the form of a spherical segment.
– An explosive charge (BP) is placed inside the case – an explosive mixture with a density of ρ = 1660 kg/m^3 and a detonation velocity D = 8000 m/s, composed of 1,3,5-trinitro-1,3,5-triazinane (hexogen, RDX) 64% and 2,4,6-trinitrotoluene (TNT) 36%, which according to its energy characteristics is a close analogue of phlegmatized RDX (ρ = 1.67 g/m^3, D = 8000 m/s).
– They have axial symmetry, which allows numerical modelling of the functioning process in a two-dimensional axisymmetric setting.

Simulation of different methods of initiation of the detonation of an explosive charge was carried out at a point on the axis of symmetry near the inner end surface of the charge body (*i.e.* in the absence of an explosive lens) and in a circle on the outer end surface of the charge (*i.e.* in the presence of an explosive lens). The point of initiation in the calculation models was located on the axis of symmetry – item 1 (without a lens) and at a distance of 46 mm away from it, towards the inner surface of the charge case – item 2 (with a lens).

The presence of axial symmetry in the construction of shaped charges considered in this work allows the use of hydrocode. The hydrocode is based on the system of equations of the mechanics of a continuum medium in Euler cylindrical coordinates for detonation products (DP) and the Prandtl-Reiss plastic flow equation for metallic structural elements [28]. This system of equations in practical implementation is replaced by an equivalent system in a two-dimensional axisymmetric formulation in a cylindrical coordinate system (r, z) using end-to-end calculation through contact boundaries according to the concentration method algorithm [29].

$$\frac{\partial \rho}{\partial t} + \frac{\partial (\rho u_r)}{\partial r} + \frac{\partial (\rho u_z)}{\partial z} + \frac{\rho u_r}{r} = 0 \tag{1}$$

$$\rho \frac{du_r}{dt} = \rho \left(\frac{\partial u_r}{\partial t} + u_r \frac{\partial u_r}{\partial r} + u_z \frac{\partial u_r}{\partial z} \right) = \frac{\partial \sigma_{rr}}{\partial r} + \frac{\partial D_{\sigma_{rz}}}{\partial z} + \frac{1}{r} \cdot \left(2 D_{\sigma_{rr}} + D_{\sigma_{zz}} \right) \tag{2}$$

$$\rho \frac{du_z}{dt} = \rho \left(\frac{\partial u_z}{\partial t} + u_r \frac{\partial u_z}{\partial r} + u_z \frac{\partial u_z}{\partial z} \right) = \frac{\partial \sigma_{zz}}{\partial z} + \frac{\partial D_{\sigma_{rz}}}{\partial r} + \frac{1}{r} \left(D_{\sigma_{rz}} \right) \tag{3}$$

$$\sigma_{rr} = D_{\sigma_{rr}} - p \;\; ; \; \sigma_{zz} = D_{\sigma_{zz}} - p \; ; \; \sigma_{rz} = D_{\sigma_{rz}} \tag{4}$$

$$\frac{dD_{\sigma_{rr}}}{dt} = 2G \cdot \left(\frac{\partial u_r}{\partial r} + \frac{1}{3\rho} \cdot \frac{\partial \rho}{\partial t} \right) + \delta_{rr} \tag{5}$$

$$\frac{dD_{\sigma_{zz}}}{dt} = 2G \cdot \left(\frac{\partial u_z}{\partial z} + \frac{1}{3\rho} \cdot \frac{\partial \rho}{\partial t} \right) + \delta_{zz}; \frac{dD_{\sigma_{rz}}}{dt} = 2G \cdot \left(\frac{\partial u_r}{\partial z} + \frac{\partial u_z}{\partial r} \right) + \delta_{rz} \tag{6}$$

$$\begin{gathered} \delta_{rr} = \left(\frac{\partial u_r}{\partial z} - \frac{\partial u_z}{\partial r} \right) \cdot D_{\sigma_{rz}}; \delta_{zz} = \left(\frac{\partial u_z}{\partial r} - \frac{\partial u_r}{\partial z} \right) \cdot D_{\sigma_{rz}}; \\ \delta_{rz} = \frac{1}{2} \cdot \left(\frac{\partial u_z}{\partial r} - \frac{\partial u_r}{\partial z} \right) \cdot \left(D_{\sigma_{rr}} - D_{\sigma_{zz}} \right) \end{gathered} \tag{7}$$

where σ_{rr}, σ_{zz}, σ_{rz}, u_r, u_z are stress and velocity components, p is the pressure and ρ is the density.

The plastic flow equations in the numerical implementation were replaced by the Wilkins procedure using Gooke's relations [30].

The Mises flow condition for an ideal plastic medium has the form:

$$D_{\sigma_{rr}}^2 + D_{\sigma_{zz}}^2 + D_{\sigma_{rz}}^2 + D_{\sigma_{rr}} \cdot D_{\sigma_{zz}} \leq \frac{2}{3} Y^2 \tag{8}$$

where the stress deviator components are $D_{\sigma_{rr}}, D_{\sigma_{zz}}, D_{\sigma_{rz}}$.

The system of equations written above is supplemented by the ratio of conservation of concentration:

$$\frac{\partial(\omega\,\rho)}{\partial t} + \frac{\partial(\rho\,\omega\,u_r)}{\partial r} + \frac{(\rho\,\omega\,u_z)}{\partial z} + \rho \cdot \frac{\omega\,u_r}{r} = 0 \tag{9}$$

Within the flow field of gas (detonation products, air) and metal in the calculated Euler element, the presence of one of the two or a part of each of the media was determined using the concentration parameter ω:

$$\omega = \frac{m_i}{m} = \begin{cases} 1, \text{ for detonation products or air} \\ 0, \text{ for body metal} \end{cases} \tag{10}$$

where m_i is the mass of explosive, DP or air, m is the mass of the Euler element.

Together with the material of the liner, a number of historical variables are transferred through the stationary Euler grid, which characterize the state and history of the deformation of the material particles. Therefore, the method of "frozen" markers was used to track the speed of movement of various parts of the structure during the explosion. "Frozen" markers are special reference points that move together with the environment in which the parameters of the current state of p_m are determined (ρ, p, u_r, u_z).

The explosion process was simulated with the help of the authors' program "Hephaestus" and the ANSYS/AUTODYN program [31-36]. To solve the given problem of mathematical assessment of the SC functioning parameters, the equation of dynamic compressibility of the liner material was used - shock adiabat in the form of Theta: $p = p(\rho)$

$$p = A\left[\left(\frac{\rho}{\rho_0}\right)^n - 1\right] \tag{11}$$

where ρ is the current value of the metal density, *A, n* are material parameters, in particular for monolithic copper $A = 30.2$ GPa, $n = 4.8$ and $\rho_0 = 8940$ kg/m^3 [28].

The detonation products (DP) of an explosive charge (EM) have other forms of the equation of state. One of the universally well-known DP state equations is the equation in the form of Jones-Wilkins-Lee (JWL) [36], which was used in this work:

$$p = A\cdot\left(1-\frac{\omega}{R_1\cdot V}\right)\cdot e^{-R_1\cdot V} + B\cdot\left(1-\frac{\omega}{R_2\cdot V}\right)\cdot e^{-R_2\cdot V} + \frac{\omega\cdot E_0}{V} \tag{12}$$

where:

- p, E_0 are pressure, and internal energy DP, respectively.
- $\bar{V} = \frac{\rho_0}{\rho}$ is the relative volume of DP,
- ρ_0, ρ are the initial and current values of the density, respectively, and
- *A, B, R1, R2, ω are*– parametric constants of the JWL equation that depend on BP.

When performing mathematical calculations, the assumption that the DP expansion process is isentropic is sometimes accepted. Therefore, instead of the equation of state, the DP isentropic equation is used, in the form of Jones-Wilkins-Lee (JWL):

$$p = p(\rho)$$

$$p_s = A \cdot e^{-R_1 \bar{V}} + B \cdot e^{-R_2 \bar{V}} + C \cdot \bar{V}^{-(\omega+1)} \quad (13)$$

where A, B, C, R_1, R_2 and ω are parametric constants of the DP isentrope.

According to [37], the values of the parametric constants of the JWL equation were taken as: A = 758.1 GPa, B = 8.513 GPa, C = 1.143 GPa, R_1 = 4.9, R_2 = 1.1 and ω = 0.2.

In addition, the mathematical model of the problem contains a medium, such as air. The function describing its behaviour uses an equation in the form of a polynomial of the form:

$$p_s = C_0 + C_1 \cdot \beta + C_2 \cdot \beta^2 + C_3 \cdot \beta^3 + (C_4 + C_5 \cdot \beta + C_6 \cdot \beta^2), \quad \beta = \frac{\rho}{\rho_0} - 1 \quad (14)$$

The coefficients of the Equation 14 (C_0, C_1, C_2, C_3, C_4, C_5 and C_6) were chosen in accordance with recommendations [38, 39].

3 Results of Studying the SCJ Free Flight Behaviour and the Interaction between the SC and a Target

Data for the SCJ velocity for tapered copper liners of progressive thickness and both small and large calibers 26 and 36.6 mm, respectively, were obtained in earlier experiments [18] and were found to be 4.367 and 5.43 km/s, respectively. This paper also described the results of ballistic experiments to determine the penetration depth of an SCJ target during a larger caliber SC explosion (Figure 2). The main results of modelling the behaviour of charges with different liners are shown in Figures 9 and 10, and in Tables 1-4. The figures show the distribution of the axial velocity of the liner material that has passed into the SCJ. The graphs were created for SCs of different geometries.

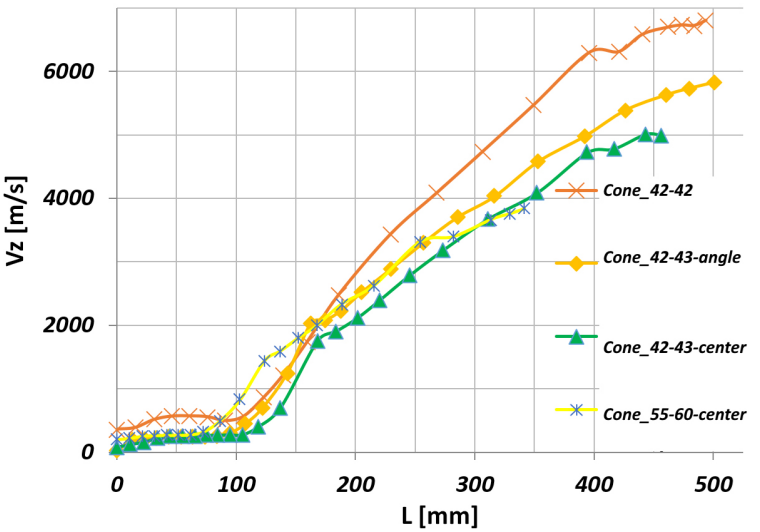

Figure 9. Distribution of axial velocity values along the SCJ for conical liners

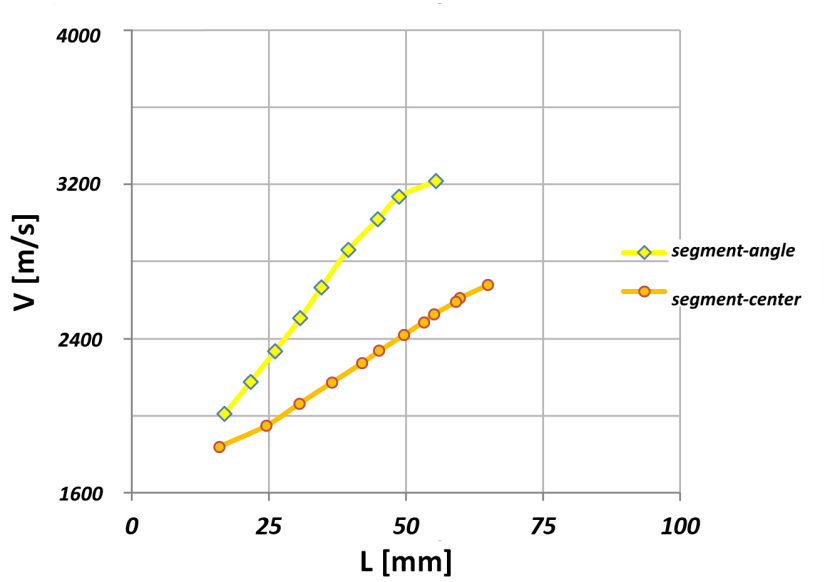

Figure 10. Distribution of axial velocity values along the SCJ for a spherical segment

Table 1. Calculated values of the gradient of axial velocity values along the SCJ length

Name of calculation scheme	Velocity gradient value V_z along the SCJ $[\frac{m/s}{mm}]$
Cone_42-42-circle	20…21
Cone_42-43-circle	14…15
Cone_42-43-center	13…14
Cone_55-60-center	11…12
Segment - circle	45…46
Segment - center	23…24

Table 2. Summary of results of simulation of the process behaviour of SCs with liners in the form of a cone under various conditions of charge detonation initiation

The shape of the cumulative funnel	Cone vertex angle [deg.]	δ [mm]	Detonation initiation method	Head velocity at initial stage of SCJ formation [m/s]		Velocity of the head at the late stage of formation of the SCJ [m/s] Calculation	Velocity of the rear of the SCJ [m/s] Calculation	Length of SCJ [mm]
				Calculation	Experiment			
Conical, constant thickness	42	1.5	circular	7700	7800	6800	550	490
Conical, progressive thickness	42 and 43	3-4		6700	–	5800	240	500
			axial	5990	5430	5000	260	450
	55 and 60			4600	4367	3800	270	340

Table 3. Results of simulation of the process behaviour of a shaped charge with liners in the form of a spherical segment under different conditions of initiation of detonation of the explosive charge

Detonation initiation method for SC	Velocity of the head of the SCJ [m/s]	Velocity of the head SCJ [m/s]	Velocity of the rear of the SCJ [m/s]	Length of SCJ [mm]
Axial	2680	2300*)	1840	50…60
Circular	3300	3400*)	2000	45…55

*) Taken from Ref. [15]

Table 4. Geometrical parameters of spherical segments and EFP rates from different sources

h/d_c	δ/d_c	Detonation velocity [m/s]	EFP velocity [m/s]	Ref.
0.183	0.021	8000	2680	this work
0.138	0.025	7980	2670	[15]
0.186	0.066	8800	1563	[19]*)
0.184	0.0375	8100	1800	[20]*)
0.215	0.0363	7980	2650	[40]

*) Charge without a shell, detonation scheme - from a point on the axis of symmetry

The graphs show that SCJs are high-velocity flows of matter, with gradients that depend on the configuration of the liner and the method of detonation initiation (Table 1). Comparison of the speed of movement of the head of the SCJ with experimental data was carried out using the results published in [16, 18]. The porosity of copper at the top of the liners did not exceed 10-11% [18]. Thus, according to [16], this value for a charge with a caliber of 81 mm with a conical copper liner of a constant thickness of 1.90 mm, and with a charge detonation velocity of 7.8 km/s, was 7.92 km/s. At a detonation velocity of 8.02 km/s, the SCJ velocity was 8.0 km/s. Thus, the detonation velocity of the SC in the experiments was 7.8-8.1 km/s, and in the mathematical calculations it was 8 km/s. Comparing the calculated results with the experimental ones (Table 2), we can conclude that the values of these results are quite close. Analyzing the results of calculations for a spherical segment, Figures 8, 10 and Table 3, we can draw the following conclusions. The velocity distribution along the SCJ in [1] is close to linear, as in Figure 10. The data from [1, 16] testify to the influence of the detonation velocity on the SCJ velocity. Thus, according to [16], a decrease in the detonation velocity of 500 m/s from 8.02 to 7.47 km/s leads to a decrease in the SCJ velocity of about the same amount, 500 m/s.

To compare the results of calculations for a spherical segment for an annular detonation scheme, we used the data obtained in [15]. In the present work, we studied a copper liner with a cone angle of ≈155° and an arch-shaped apex. Charge (explosive 8701, D = 7.98 km/s) the diameter of 60 mm and the height of 45 mm. The body of the SC was made of Steel 45. It should be noted that for such an SC, the difference between the calculated and experimental values of the velocity of the SCJ is insignificant: 3400 and ≈3300 m/s (Figure 10, Table 3). Here the difference between the calculated results and the known experimental data can be seen. For an SC with a spherical segment, in the detonation scheme of the SC charge at a point on the axis of symmetry: 2680 and 2300 m/s [15], respectively (Table 3). Most of the published papers reported that the experimental values of the speed of copper EFPs (explosively formed penetrators) were in the range of ≈1500-2600 m/s. This difference between the calculated and experimental velocities can be explained by geometric differences in the shape and thickness of the liner, as well as in the shape of the SC charge [15]. Table 4 lists some data from various sources about liners that form explosively formed penetrators during an explosion. To some extent, they confirm this observations.

4 The Results of Calculations of SCJ Penetration into a Target According to the AV Model and Their Comparison with Experimental Values

In [21], a rule for the approximate determination of the possible velocity of a continuous, unbroken SCJ was formulated: the maximum possible velocity of the jet tip V_0 is 2.34 higher than the volume velocity of sound in the liner material. Based on this rule, in the present work, the ranking of metals was carried out according to the criterion $V_0\sqrt{\rho_j}$ (ρ_j is the density of the SCJ material). As a result of this ranking, the first places are occupied by W, Mo, Ni, Cu, respectively. This analysis explains, for example, the velocity characteristics of molybdenum and tungsten SCs, which exceed those of similar lighter copper ones [22]. Consider the data for 70/30 and a conical liner with an apex angle of $2\alpha = 42°$. The main parameters for Cu, Mo, W [22] are:

– velocity of the front part of the SCJ, V_0, are respectively: 8400-8500, 11250-11650 and 8490-9330 m/s,
– SCJ destruction start time from the moment the detonation wave reaches the liner surface (break-up time) are respectively: – t_b = 149-193, 87-122 and 114-123 μs, – ratio t_b/D = 1.84-2.38, 1.19-1.60 and 1.41-1.52.

The advantages of copper SCJs over Mo and W are: longer time to failure;

simple manufacturing technology and cost. However, the question arises: which material should be preferred for the maximum penetration depth of an SCJ in practical applications? To answer this question, we used a special model. The model differs from hydrodynamic theory and its modifications. The model takes into account the main physical effects that affect the penetration depth (L): SCJ velocity, velocity gradient along the SCJ, the influence of the distance from the charge to the target and the difference in the density of the materials of the SCJ and the target. The model proposed by Allison and Vitali (model A-V), and the formulas obtained by Dipersio and Simon on the basis of this model are given explicitly in [23]. Model A-V considers different options:

– penetration without breaking of the SCJ ($t<t_b$, tb is the break up time of of the SCJ),
– destruction of the SCJ upon penetration into the barrier ($t_0 < t_b \leq t$),
– destruction of the SCJ before penetration into the barrier t_0 ($t_b \leq t_0 \leq t$).

For the first two variants, the formulas for the penetration depth are as follows:

$$L = z_0 \left[\left(\frac{V_0}{V_c} \right)^{\frac{1}{\gamma}} - 1 \right] \tag{15}$$

$$0 \leq z_0 < V_c t_b \left(\frac{V_c}{V_0} \right)^{\frac{1}{\gamma}} \tag{16}$$

$$L = \frac{(1+\gamma)(V_0\, t_b)^{\frac{1}{(1+\gamma)}} Z_0^{\frac{\gamma}{(1+\gamma)}} - V_c t_b}{\gamma} - Z_0 \tag{17}$$

$$V_c t_b \left(\frac{V_c}{V_0} \right)^{\frac{1}{\gamma}} \leq z_0 < V_0 t_b \tag{18}$$

where V_c is the velocity of the SCJ element at which its penetration into the barrier stops, $\gamma = \sqrt{\rho_t/\rho_j}$ (where ρ_t is the density of the target material and ρ_j is the density of the SCJ material).

According to the hydrodynamic theory, $L = (1/\gamma)z_0$ does not depend on the velocity gradient along the SCJ. At the same time, in many reports, including this one, it is shown that the velocities of the elements decrease from the front to the tail parts of the SCJ. The parameter t_b also varies along the SCJ [24]. For a charge with a caliber of 63 mm and an angle at the cone apex of 48°42′, the parameter t_b varied from 120 μs at the front of the SCJ to 210 μs at the tail, which

is close to these values from [22].

Calculations by Equation 17 for high-strength steel with V_c = 3000 m/s and z_0 = 300 mm, showed that the penetration depth of a copper SCJ is 530.9 mm, and that of a molybdenum SCJ is 620.1 mm. That is, despite the larger value of the parameter t_b for copper, a molybdenum SCJ has an advantage over copper. If the value of t_b is such that the copper SCJ penetrates the target before breaking, then the penetration depth is determined by Equation 15, and is 612 mm. The difference in this case is small. The depth of penetration will ultimately be determined by the quality of the material (cleanliness and grain size), as well as the accuracy of liner manufacture [1, 11, 16]. In the calculations, the corresponding parameters had the following values:

– for Cu: t_b = 150 μs and V_0 = 8500 m/s,
– for Mo: t_b = 90 μs and V_0 = 11300 m/s.

Calculations using Equation 15 give the following results L for z_0 = 60 mm: 122 mm (Cu) and 213.1 mm (Mo).

For comparison, let us consider the known experimental data obtained during testing of shaped-charge perforator charges for the oil and gas industry [18]. In an SC burst with a tapered liner of progressive thickness and apex angles of 43° and 45°, the front velocity of the SCJ was 5430 m/s. The calculation of L by Equation 15 for z_0 = 50 and 75 mm, V_c = 2000 m/s (low carbon steel) is 87 and 130.5 mm, respectively. The experimental data obtained by the method described in [18] for z_0 = 50 mm were 92-101 mm. For a 44° and 48° apex liner, the SCJ velocity was 6170 m/s. The penetration depth of steel in these experiments with:

– z_0 = 21 mm was 74-80 mm (calculation by Equation 15 gave 45.2 mm),
– z_0 = 34 mm was 80-85 mm (calculation by Equation 15 gave 73.2 mm).

That is, there is a relatively satisfactory agreement between the experimental and calculated data, but the accuracy of the calculations decreases as the value of z_0 decreases. It is likely that this value in the calculations should be the so-called focal length – the distance to the target at which the penetration value will be a maximum. For short-focus charges, it is at least 1-2 charge calibers. Note that calculations using Equation 15 for small values of the distance between the charge and the target ($\leq 0.5d_c$) give underestimated values compared to the experimental data. So, for industrial charges with a caliber d_c = 26 mm, the distance to the barrier was 10 mm, respectively, and 20 mm, numerous experimental data were obtained. In tests of industrial batches on targets made of steel St.3, the distance to the barrier was 50...55 and 72...75 mm, respectively. These differ significantly from the calculated ones (13.2 and 26.4 mm). This theory therefore has a limited range of application, namely: for fully formed SCJs and charges located at a distance from the target of $z_0 \geq (1\text{-}2)d_c$. In this case, in order to select

the calculation by Equation 15 or 17 it is necessary to determine the value of tb by experiment. The dependence of this quantity on the SC caliber has not been studied. According to physical considerations and criteria of the theory of similarity, the time intervals should decrease with decreasing caliber. According to [1], the velocity, density, and pressure in flows of the same substance from charges of different calibers will be the same under the following condition: $Dt/d_c = const$, where t is the time of formation, free flight, and time to destruction of the SCJ, t_b. In the case of the geometric similarity of two charges of different calibers but of the same explosive material, the ratio of the time intervals is determined by the ratio of the characteristic dimensions, in this case, calibers: $t_1/t_2 = d_{c1}/d_{c2}$. Therefore, the SCJ in the explosion of charges of small calibers is destroyed earlier than in the explosion of charges of large calibers. The velocity of the SCJ during explosions of geometrically similar charges of different calibers will be the same, but at different times.

5 Discussion of Results of Studying the SCJ Free Flight Behaviour and the Interaction Between the SC and the Target

It should be emphasized that the effect of a decrease in the SCJ velocity in the initial stage of its formation (Table 2) was also observed by other authors [12, 15, 25]. The influence of the number and location of the initiation points on the kinetic and geometric parameters of the explosively formed penetrator was studied in [15]. The magnitude of the velocity reduction in [15] did not exceed 50-60 m/s. Obviously this is due to the shape of the liner. In [12], this decrease for liners made of an amorphous ZrCuNiAlAg alloy with an eccentric geometric figure in the form of two symmetrical hemispheres reached almost 500 m/s. The average reduction was about 300 m/s. It was also shown in [15] that that the location of the initiation points and their number affects the speed of the projectile element (EFP) and its geometric characteristics (length to diameter ratio). One of the positive effects found in the numerical experiments in [15] is an increased length-to-diameter ratio for symmetrical detonation initiation from two points, compared to a non-symmetrical arrangement of one, two, or three points of detonation excitation. The effect of elongation of a compact element (explosively formed penetrator) upon changing the detonation pattern from point to circular in the presence of an inert lens was observed in the numerical experiments performed, as well as in [5]. In [12], the authors observed an increase in the speed of the SCJ front from 4600 to 4750 m/s with a decrease in the radius of curvature from 110 to 90 mm with a liner wall thickness of 2.6 mm and an

eccentricity of 37 mm. Decreasing the lining thickness, δ, from 3.8 to 1.4 mm led to an increase in the SCJ velocity from ≈4200 to ≈5600 m/s (for a lining curvature radius of 100 mm and an eccentricity of 37 mm). The maximum decrease in the SCJ velocity (≈350 m/s) occurred with the thickest lining.

The effect of an increase in the velocity of the SCJ and the EFP, the dimensions of the EFP, and the depth of penetration into the target during the transition from the point scheme of detonation initiation to the scheme of radial or annular initiation, should be noted. This increases not only the speed of the SC, but also its length. Thus, according to the data in [15], the speed increases from 2300 to 3400 m/s. According to calculations (Table 3), the increase occurs from 2680 m/s to ≈3300 m/s. The largest difference in SCJ velocity for different initiation schemes was obtained for a conical aluminum liner with a 90° apex angle: 5000 and 12000 m/s, respectively [27]. The length of the explosively formed penetrator gradually increases with increasing radius of the initiation loop. The increase in the EFP length upon reaching the radius of the initiation contour equal to half the charge caliber is almost tenfold [15]. The penetration depth of an EFP during point detonation on the axis of symmetry reaches 0.65 times the charge caliber. The penetration depth of the EFP during circular detonation and with the radius of its contour of 0.333 caliber, reaches 1.24 times the caliber of the charge. With a contour radius of 0.5 caliber charge, the penetration depth reaches 1.55 caliber.

It is of practical interest to obtain a single dependence $V_0(2\alpha)$ for conical copper liners with different angles at the vertices. Such a dependence can be very useful when designing various devices using SCs. It allows the liner configuration to be selected to obtain the desired penetration result. To plot the dependence of $V_0(2\alpha)$ for the cone, we used the experimental and calculated data on V_0 from [16, 18] (dots on the left and in the middle, respectively). The experimental and calculated data were augmented by the results of modelling and experiments for cone-shaped segments with obtuse angles ≥140° and low-spherical segments close to them in shape [15, 19, 20, 40-42] (point on the right) (Figure 11).

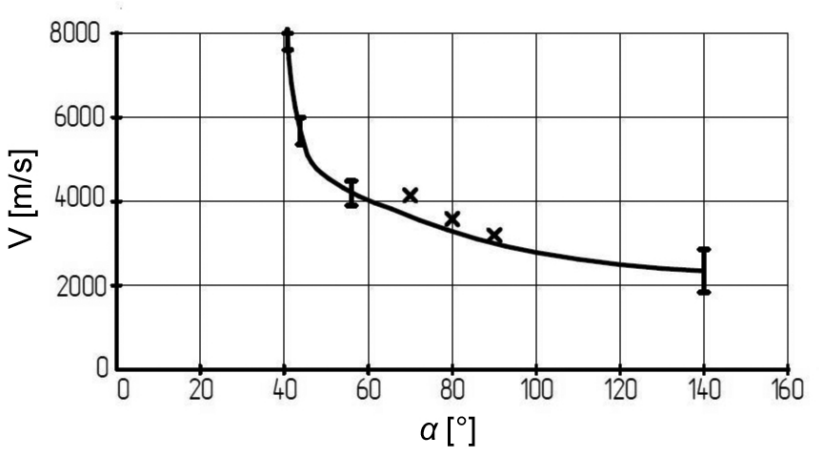

Figure 11. Copper SCJ velocity as a function of the angle at the apex of the conical liner

About gradient materials for liners of SCs. The articles [18, 26] investigated the distribution of porosity in the materials copper, aluminum and composite (W-Cu-Pb) of conical liners from the top to the base. The liners were made from powdered materials by cold pressing. It was shown that the porosity of the material at the top of the copper liner was ≈2.6...2.8 times lower than at the base (10% and 26...28%, respectively). For the composite porous material, this difference was smaller and amounted to 1.25...1.3. All of the physical and mechanical properties of the materials depend on the porosity of the material, so it can be assumed that these products are made of materials with gradient properties. At the same time, the speed of sound decreases from the top of the liner to the base. Given that the jet velocity is correlated with the speed of sound, materials such as Mo and W are preferred for making the SC tip, or their mixtures (pseudoalloys) with other metals (Cu, Ni, Pb). In [16], the process of bursting of hemispherical and conical liners made of nickel and copper layers was studied experimentally and by computer modelling. This idea can be productive for designing liners with gradient materials using other metals. Note that the number of publications in which materials with gradient properties are studied is quite limited [6, 16, 18, 21, 26]. As a rule, in studies of the behaviour of charges by mathematical modelling, the change in the porosity and density of the material along the generatrix of the liner is not taken into account, although the effect of porosity and its gradient along the liner was observed experimentally [43, 44].

6 Conclusions

- Suggested modelling methods and computational procedures have shown results that are in satisfactory agreement with the known data from experimental and computational studies. These data can be used to optimize charge designs in practical applications.
- The engineering theory of Dipersio and Simon based on the A-V model satisfactorily describes the penetration depth of a target made of steel St.3 and copper SC (for the case of a small distance between the charge and the target (1-2) caliber). For small distances between the SC and the target (< 1 caliber), other models and calculation methods are required.
- The dependence of the velocity of the leading part of a copper SCJ on the angle at the top of the conical liner, for a detonation velocity of 7.8-8 km/s, was obtained. The velocity dependence obtained is close in form to a power function.
- The dependence of the velocity of the elements along the SCJ is close to linear, and the slope of the curve depends on the shape and thickness of the liner.

Acknowledgements

The authors thank Bugayets V.P. for help in carrying out the experiments. The experiments were carried out with the support of the State Geological Service of Ukraine and the company “Ukrgazvydobuvannya”.

References

[1] Babkin, A.V.; Kolpakov, V.I.; Ladov, S.V.; Orlenko, L.P. The Shaped Charge Effect (in Russian) In: *The Physics of Explosion.* Vol. 2, **2004**, pp**.** 389-524**.**

[2] Ou, J.-H.; Ou, J.-B.; Jhu, Y.-J. The Design and Analysis for Shaped Charge Liner Using Taguchi Method. *Int. J. Mech.* **2014**, *8*: 53-61.

[3] Pyka, D.; Kurzawa, A.; Bocian, M.; Bajkowski, M.; Magier, M.; Sliwinski, J.; Jamroziak, K. Numerical and Experimental Studies of the ŁK Type Shaped Charge. *Appl. Sci.* **2020**, *10*: paper 6742; http://dx.doi.org/10.3390/app10196742.

[4] Zhang, X.-f.; Qiao, L. Studies on Jet Formation and Penetration for a Double-layer Shaped Charge. *Combust. Explosion Shock Waves* **2011**, *47*: 241-248; https://doi.org/10.1134/S0010508211020134.

[5] Tymoshenko, A.B.; Chepkov, I.B. Modeling of the Functioning of Warhead Containing Projectile-forming Elements. *Military and Technical Collection* **2011**, *2*(5): 73-81.

[6] Habera, Ł.; Hebda, K.; Koślik, P.; Sałaciński, T. The Shooting Tests of Target Perforating Ability, Performed on Cast Concrete Cylinders. *Cent. Eur. J. Energ. Mater*. **2020**, *17*(4): 584-599; https://doi.org/10.22211/cejem/132066.
[7] Elshenawy, T.; Li, Q.-m.; Elbeih, A. Experimental and Numerical Investigation of Zirconium Jet Performance with Different Liner Shapes Design. *Def. Technol.* **2022**, *18*(1): 12-25; https://doi.org/10.1016/j.dt.2020.11.019.
[8] Kemmoukhe, H.; Savić, S.; Terzić, S.; Lisov, M.; Rezgui, N.; Sedra, H. Improvement of the Shaped Charge Jet Penetration Capability by Modifying the Liner Form Using AUTODYN-2D. *Sci.-Tech. Rev.* **2019**, *69*(1): 10-15; https://doi.org/10.5937/str1901010K.
[9] Fedorov, S.V. Numerical Simulation of the Formation of Shaped-charge Jets from Hemispherical Liners of Degressive Thickness. *Combust. Explosion Shock Waves* **2016**, *52*: 600-612; https://doi.org/10.1134/S0010508216050117.
[10] Du, Y.; He, G.; Liu, Y.; Guo, Z.; Qiao, Z. Study on Penetration Performance of Rear Shaped Charge Warhead. *Materials* **2021**, *14*: paper 6526; https://doi.org/10.3390/ma14216526.
[11] Minin, V.F.; Minin, I.V.; Minin, O.V. Physics Hypercumulation and Combined Shaped Charges. *Proc. 11th Int. Conf. on Actual Problems of Electronic Instrument Engineering* (*APEIE*) – 30057, Vol. 1, NSTU, Novosibirsk, **2012**, pp. 34-52; http://doi.org/10.1109/APEIE.2012.6628935.
[12] Cui, P.; Shi, D.; Xu, J.; Wang, T.; Zhang, Z.; Li, Z.; Wang, D. Numerical Simulation on Jet Forming and Penetration Performance of Several Amorphous Energetic Alloy Liner with Typical Structures. *J. Phys.: Conf. Ser. 1948,* **2021,** 012186 IOP Publishing, http://doi.org/10.1088/1742-6596/1948/1/012186.
[13] Elshenawy, T.; Elbeih, A.; Li, Q.M. Influence of Target Strength on the Penetration Depth of Shaped Charge Jets into RHA Targets. *Int. J. Mech. Sci.* **2018**, *136*: 234-242; https://doi.org/10.1016/j.ijmecsci.2017.12.041.
[14] Markelov, G.E. Effect of Initial Heating of Shaped Charge Liners on Shaped Charge Penetration. *J. Appl. Mech. Tech. Phys.* **2000**, *5*: 788-791; https://doi.org/10.1007/BF02468723.
[15] Li, W.; Wang, X.; Li, W. The Effect of Annular Multi-point Initiation on the Formation and Penetration of an Explosively Formed Penetrator. *Int. J. Impact Engineering* **2010**, *37*: 414-424; https://doi.org/10.1016/j.ijimpeng.2009.08.008.
[16] Walters, W. *Introduction to Shaped Charges.* Aberdeen Proving Ground, MD 21005-5069, Army Research Laboratory. ARL-SR-150, **2007**, p. 110.
[17] Resnyansky, A.D.; Katselis, G.; Wildegger-Gaissmaier, A.E. Experimental and Numerical Study of the Shaped Charge Jet Perforation against Concrete Target. *CD-ROM Proc. 21st Int. Symp. Ballistics,* additional entries, **2004**.
[18] Drachuk, A.G.; Goshovskii, S.V.; Voitenko, Y.I. *The Calculation Parameters of Shaped Charges with Porous Liners.* (in Ukrainian) Ukrainian State Geological Exploration Institute, Kiev, **2007**, p. 42
[19] Wua, J.; Liu, J.; Du, Y. Experimental and Numerical Study on the Flight and Penetration Properties of Explosively-formed Projectile. *Int. J. Impact Engineering*

2007, *34*(7): 1147-1162; https://doi.org/10.1016/j.ijimpeng.2006.06.007.
[20] Kolpakov, V.I.; Savenkov, G.G.; Rudometkin, K.A.; Grigor'ev, A.Yu. Numerical Simulation of the Formation of Compact Strikers from Low-Sphericity Linings. *Tech. Phys.* **2016**, *61*(8): 1141-1145; https://doi.org/10.1134/S1063784216080156.
[21] Held, M. Liners for Shaped Charges. *J. Battlefield Technol.* **2001**, *4*(3): 1-6.
[22] Pham, J.D.; Baker, E.L.; De Fisher, S. *Shaped Charge Jet Flash Radiography Digitization.* Technical Report ARAET-TR-05013, US Army Armament Research, Development and Engineering Center, Picatinny, New Jersey, **2005**, p. 39.
[23] Simon, J.; Dipersio, R.; Merendino, A.B. *Penetration of Shaped-Charge Jets into Metallic Targets; Ballistic Research Laboratory Memorandum.* Report No. 1296; Ballistic Research Laboratory, Aberdeen, US-MD, **1965**.
[24] Petit, J.; Jeanclaude, V.; Fressengeas, C. Break-up of Copper Shaped-charge Jets: Experiment, Numerical Simulations, and Analytical Modelling. *J. Appl. Phys.* **2005**, *98*: paper 123521; http://dx.doi.org/10.1063/1.2141647.
[25] Salkičević, M. Numerical Simulations of the Formation Behavior of Explosively Formed Projectiles. *Defense Security Studies* **2022**, *3*: 1-14; https://doi.org/10.37868/dss.v3.id183.
[26] Voitenko, Y.I.; Goshovskii, S.V.; Drachuk, A.G.; Bugaets, V.P. Mechanical Effect of Shaped Charges with Porous Liners. *Combust. Explos. Shock Waves* **2013**, *49*(1): 109-116; https://doi.org/10.1134/S0010508213010127.
[27] Murphy, M.J. *Shaped-Charge Penetration in Concrete: A Unified Approach.* Doctor Dissertation, University of California, Livermore, California, **1983**, p. 114.
[28] Orlenko, L.P.; Selivanov, V.V. An Explosion in Solids. (in Russian) In: *The Physics of Explosion.* Vol. 2, **2004**, pp. 389-524.
[29] Calculation of Gas-dynamic Flows Based on the Concentration Method. (in Russian) (Bakhrach, S.M.; Gogoleva, Yu.P.; Samygulin, M.S.; Eds.) *Dokl. Academy of Sciences of the USSR* **1981**, *257*(3): 566-569.
[30] *Numerical Methods in Problems of Physics of Explosion and Impact*. (in Russian) (Babkin, A.V.; Kolpakov, V.I.; Okhityn, V.N.; Eds.) textbook for students, Vol. 3, Moscow State Technical University, Russia, **2000**, p. 516.
[31] Odintsov, V.A.; Sydorenko, Yu.M.; Tuberozov, V.S. Modeling of the Explosion Process of a High-explosive Projectile Using a Two-dimensional Hydrocode. *Def. Technol.* **2000**, *1-2*: 49-55.
[32] Sydorenko, Yu.M. Methodology of Two-dimensional Computer Modeling of the Processes of Functioning of High-explosive Munitions. *Artillery and Gunnery* **2005**, *1*: 18-21.
[33] Sidorenko, Yu.M.; Shlenskii, P.S. On the Assessment of Stress-strain State of the Load-Bearing Structural Elements in the Tubular Explosion Chamber. *Strength Mater.* **2013**, *45*(2): 210-220.
[34] Sydorenko, Yu.; Semon, B.; Yakovenko, V.; Ryzhov, Y.; Ivanyk, E. Spatial Distribution of Mass and Speed on Movement of Two Shrapnel Discs of Variable Thickness in Explosive Load. *Def. Sci. J.* **2020**, *70*: 479-485; https://doi.org/10.14429/dsj.70.14524.

[35] Kravets, V.; Zakusylo, R.; Sydorenko, Y.; Sałaciński, T.; Zakusylo, D. Regularities of the Energy of Formation Field in the Explosion of a Conical Charge. *Cent. Eur. J. Energ. Mater.* **2019**, *16*(4): 533-546; https://doi.org/10.22211/cejem/115355.
[36] Webpage: www.ansys.com.
[37] Johnson, G.R.; Cook, W.H. Fracture Characteristics of Three Metals Subject to Various Strains, Strain Rates, Temperatures and Pressures. *Eng. Frac. Mech.* **1985**, *21*(1): 31-48.
[38] *LLNL Explosive Handbook. Properties of Chemical Explosives and Explosive Simulants.* (Dobratz., B.M.; Crawford, P.C.; Eds.) Livermore, California, **1985**, p. 541.
[39] *Mathematical Modeling of Shock and Explosion Processes in the LS-DYNA Program.* (Muizemnek, A.Yu.; Bogach, A.A.), textbook, Information and Publishing Center of Penza State University, Penza, Russia, **2005**, p. 106.
[40] Kruglov, P.V.; Kolpakov, V.I. Laws of Explosive Formation of Elongated High-speed Elements from Steel Segmental Liners. *Engineering Magazine: Science and Innovations* **2017**, 12. http://dx.doi.org/10.18698/2308-6033-2017-12-1714.
[41] Żochowski, P.; Warchoł, R. Experimental and Numerical Study on the Influence of Shaped Charge Liner Cavity Filling on Jet Penetration Characteristics in Steel Targets. *Def. Technol.* **2023**, *23*: 60-74, https://doi.org/10.1016/j.dt.2022.09.007.
[42] Żochowski, P.; Warchoł, R.; Miszczak, M.; Nita, M.; Pankowski, Z.; Bajkowski, M. Experimental and Numerical Study on the PG-7VM Warhead Performance against High-Hardness Armor Steel. *Materials* **2021**, *14*: paper 3020; https://doi.org/10.3390/ma14113020.
[43] Voitenko, Y.I.; Bugajets, V.P. Influence of Aluminum on the Impact Properties of Composite Cumulative Jets. (in Russian) *Bull. National Technical University of Ukraine «Kiev Polytechnic Institute»* **2016**, *30*: 36-48.
[44] Voitenko, Y.I.; Zakusylo, R.V.; Wojewodka, A.T.; Gontar, P.A.; Gerlich, M.M.; Drachuk, O.G. New Functional Materials in Mechanical Engineering and Geology. *Cent. Eur. J. Energ. Mater.* **2019**, *16*(1): 135-149; https://doi.org/10.22211/cejem/105598.

Received: August 1, 2023
Revised: October 3, 2023
First published online: December 21, 2023
Updated online: January 21, 2024